

# Bismuth radical catalysis in the activation and coupling of redox-active electrophiles

Received: 23 June 2022

Accepted: 3 May 2023

Published online: 1 June 2023

Check for updates

Mauro Mato <sup>1</sup>, Davide Spinnato <sup>1</sup>, Markus Leutzsch <sup>1</sup>, Hye Won Moon <sup>1</sup>, Edward J. Reijerse <sup>2</sup> & Josep Cornella <sup>1</sup>✉

Radical cross-coupling reactions represent a revolutionary tool to make C(*sp*<sup>3</sup>)–C and C(*sp*<sup>3</sup>)–heteroatom bonds by means of transition metals and photoredox or electrochemical approaches. However, the use of main-group elements to harness this type of reactivity has been little explored. Here we show how a low-valency bismuth complex is able to undergo one-electron oxidative addition with redox-active alkyl-radical precursors, mimicking the behaviour of first-row transition metals. This reactivity paradigm for bismuth gives rise to well-defined oxidative addition complexes, which could be fully characterized in solution and in the solid state. The resulting Bi(III)–C(*sp*<sup>3</sup>) intermediates display divergent reactivity patterns depending on the  $\alpha$ -substituents of the alkyl fragment. Mechanistic investigations of this reactivity led to the development of a bismuth-catalysed C(*sp*<sup>3</sup>)–N cross-coupling reaction that operates under mild conditions and accommodates synthetically relevant NH-heterocycles as coupling partners.

Metal-catalysed radical cross-coupling reactions represent a conceptual paradigm shift from the historical two-electron polar disconnections<sup>1</sup>, resulting in a new approach for the synthesis of organic molecules<sup>2</sup>. Particularly, disconnections based on the coupling of alkyl-radical fragments have been shown to hold tremendous potential in making C(*sp*<sup>3</sup>)–C and C(*sp*<sup>3</sup>)–heteroatom bonds<sup>3,4</sup>. The evolution and application of such a synthetic strategy is linked to advances in the fields of photoredox catalysis<sup>5–7</sup> and electrochemical synthesis<sup>8,9</sup> and, especially, their combination with first-row transition-metal catalysis<sup>10–13</sup>. Indeed, elements such as Fe, Co, Ni or Cu hold a preferential place when one-electron processes are required in cross-coupling cycles, resulting in redox events occurring via  $(n)/(n+1)/(n+2)$  oxidation states (Fig. 1a, right). This particular chemical behaviour leads to the facile generation of alkyl-radical fragments through single-electron transfer (SET) oxidative addition from precursors such as redox-active esters (RAEs) or Katritzky salts (KSs).

Recent years have witnessed significant efforts towards mimicking the redox behaviour of transition metals by main-group elements<sup>14</sup>. For instance, pnictogens can take part in S<sub>N</sub>2-type polar oxidative additions resulting in two-electron manoeuvring throughout  $(n)/(n+2)$  redox

catalytic cycles, emulating those of late transition metals (Fig. 1a, left)<sup>15</sup>. However, radical oxidative additions of redox-active electrophiles have generally been restricted to first-row transition metals and well-defined examples of this process with a main-group complex remain elusive<sup>6,16</sup>. Very recently, bismuth redox catalysis has been established as an emerging platform for organic synthesis<sup>17</sup> and our group has shown how Bi(III/V) or Bi(I/III) catalytic cycles can lead to the development of C–F (ref. 18), C–O (ref. 19) or C–H (ref. 20) bond-forming reactions, among others<sup>21</sup>. Nevertheless, despite the fact that persistent and stable radicals of heavier main-group elements are known<sup>22</sup>, bismuth radical catalysis has been significantly underexplored<sup>23</sup>. Bi(II/III) catalytic cycles have been postulated for the living radical polymerization of alkenes<sup>24</sup> or the cycloisomerization of 4-iodoalkenes<sup>25</sup>. This, together with further reports probing the existence of bismuth(II)-centred radicals<sup>26</sup>, prompted us to explore the behaviour of the Bi(I/II) pair in SET-based oxidative additions of redox-active alkyl electrophiles. In this Article, we show how a well-defined bismuthinidene (**1**) reacts with alkyl phthalimide esters and alkyl KSs to give alkyl-bismuth(III) adducts, which were found to behave as Bi–C radical-equilibrium complexes (Fig. 1b, bottom). Additionally, we discovered that  $\alpha$ -amino alkyl-radical

<sup>1</sup>Max-Planck-Institut für Kohlenforschung, Mülheim an der Ruhr, Germany. <sup>2</sup>Max-Planck-Institut für Chemische Energiekonversion, Mülheim an der Ruhr, Germany. ✉e-mail: [cornella@kofo.mpg.de](mailto:cornella@kofo.mpg.de)

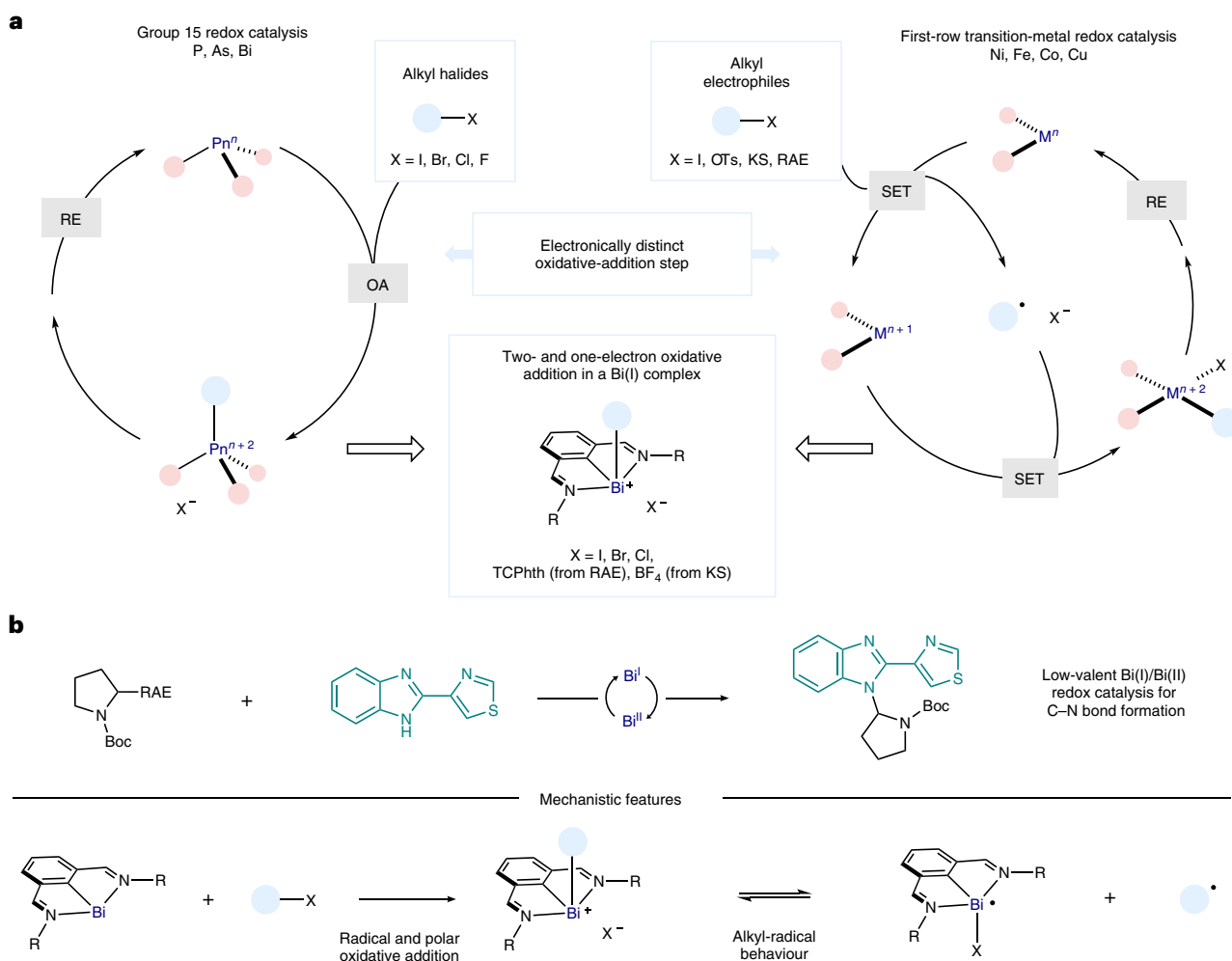


**Fig. 1 | Unlocking single-electron oxidative-addition processes for bismuth.** **a**, Merging pnictogen reactivity (left: polar, two-electron pathways dominate) with first-row transition-metal behaviour (right: radical, one-electron processes dominate) to unveil the oxidative addition of redox-active alkyl-radical

precursors to bismuth(I) via SET. **b**, Development of a bismuth-catalysed C–N cross-coupling reaction through the study of the radical behaviour of alkyl-bismuth(III) complexes. OA, oxidative addition; RE, reductive elimination; Boc, *tert*-butoxycarbonyl; Ts, 4-toluenesulfonyl; Pn, pnictogen. R = *tert*-butyl.

fragments resulting from this process can be easily oxidized by Bi(II), giving rise to iminium ions<sup>27,28</sup> that can be trapped by N-nucleophiles. This observation led to the development of a Bi-catalysed radical C–N cross-coupling reaction with a wide scope of both coupling partners (Fig. 1b, top). In spite of the vast number of alkyl-radical couplings developed during the past decade, only a few examples of C(*sp*<sup>3</sup>)–N bond formation from redox-active radical precursors have been reported<sup>29</sup>, mainly relying on photoredox set-ups<sup>30–33</sup>, electrochemical synthesis<sup>34,35</sup> or the use of an excess of chemical oxidant<sup>36</sup>. In this Article, we demonstrate that catalytic amounts of a Bi(I) complex can promote this type of transformation in an autonomous manner, without the need for a photoredox system, a chemical oxidant, an external base or an electrochemical set-up.

## Results and discussion

As a result of the high nucleophilicity of the 6*p*<sup>2</sup> lone pair on the Bi(I) centre, bismuthinidene **1** (refs. 37,38) has recently been shown to engage in polar S<sub>N</sub>2-type reactions with alkyl halides and triflates<sup>39</sup>. Similarly, **1** reacted quantitatively with a range of benzyl (pseudo)halides (Cl, Br, I, mesylate) to give benzyl bismuth(III) complexes **5–8** (Fig. 2b). Cyclic-voltammetry analysis of **1** ( $E_{1/2} = -0.85$  versus Fc<sup>0/+</sup>, the ferrocene/ferrocenium couple) provides evidence that C–X (X = halide) cleavage should proceed through a classical S<sub>N</sub>2 pathway ( $E_{p/2} < -2.0$  V versus

Fc<sup>0/+</sup>). On the other hand, the electrochemical behaviour suggested that **1** could potentially engage in SET oxidative-addition processes with alkyl redox-active electrophiles (Fig. 2a). Accordingly, reaction of **1** with 1 equiv. of tetrachlorophthalimide (TCPht) ester **2** ( $E_{p/2} = -1.2$  V versus Fc<sup>0/+</sup>) cleanly afforded benzyl bismuth(III) complex **9** after SET, fragmentation, release of CO<sub>2</sub> and radical recombination (given that the potential difference between **1** and **2** is approximately 0.35 V, SET between **1** and **2** can be estimated to be approximately 8 kcal mol<sup>-1</sup> uphill, but subsequent release of CO<sub>2</sub> can drive the oxidative-addition process)<sup>40</sup>. The resulting alkyl-bismuth(III) adduct could be fully characterized by NMR, high-resolution mass spectrometry (HRMS) and single-crystal X-ray diffraction. Furthermore, KS **4** ( $E_{p/2} = -1.3$  V versus Fc<sup>0/+</sup>) also underwent radical oxidative addition with **1** to give **10**. As expected, non-chlorinated phthalimide ester **3** ( $E_{p/2} = -2.0$  V versus Fc<sup>0/+</sup>) remained unreacted when mixed with **1**. Besides benzyl groups, the same process occurs with primary (**12**) or secondary (**13**) RAEs, leading to stable alkyl-bismuth(III) complexes. Tertiary RAEs such as the one derived from 1-adamantanecarboxylic acid did also react with **1**, but the resulting adducts were found to be unstable and could not be characterized under standard conditions. Interestingly, the process is orthogonal to classical polar transition-metal oxidative additions, as it could be performed in the presence of an aryl bromide, giving **11** as the sole product in 93% yield (Fig. 2b). This reactivity is a rare example

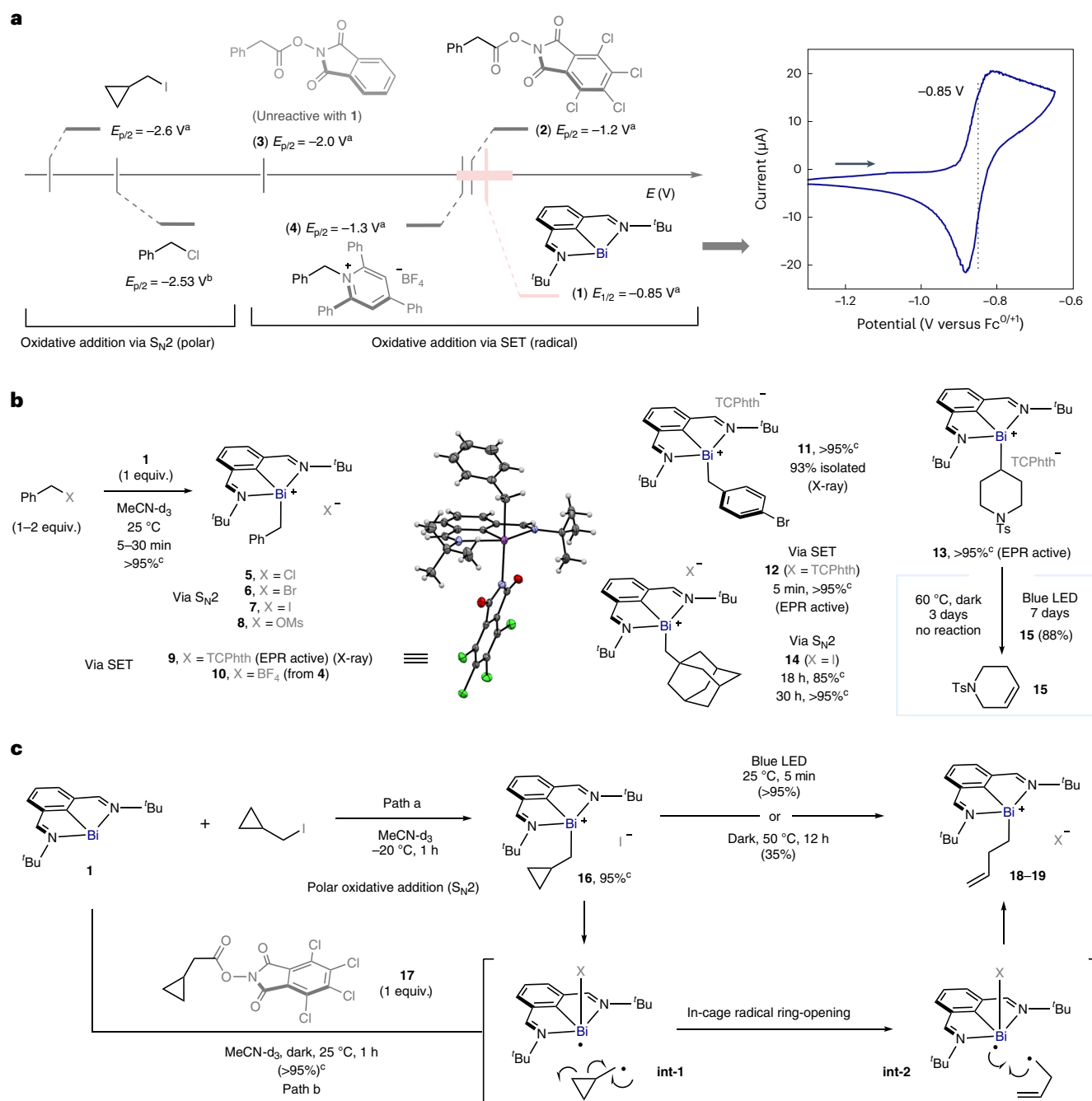


**Fig. 2 | Oxidative additions to bismuth(I).** **a**, Evaluating electronically different (polar,  $E_{p/2} < -2.0$  V, versus radical,  $E_{p/2} > -2.0$  V) oxidative additions to bismuthinidene **1** (left). Cyclic voltammometry of **1** (right). **b**, Stable oxidative-addition complexes accessed via  $S_N2$  (**5–8** and **14**) or SET (**9–13**) mechanisms. **c**, Evidence for alkyl-radical formation after oxidative addition. <sup>a</sup> Cyclic

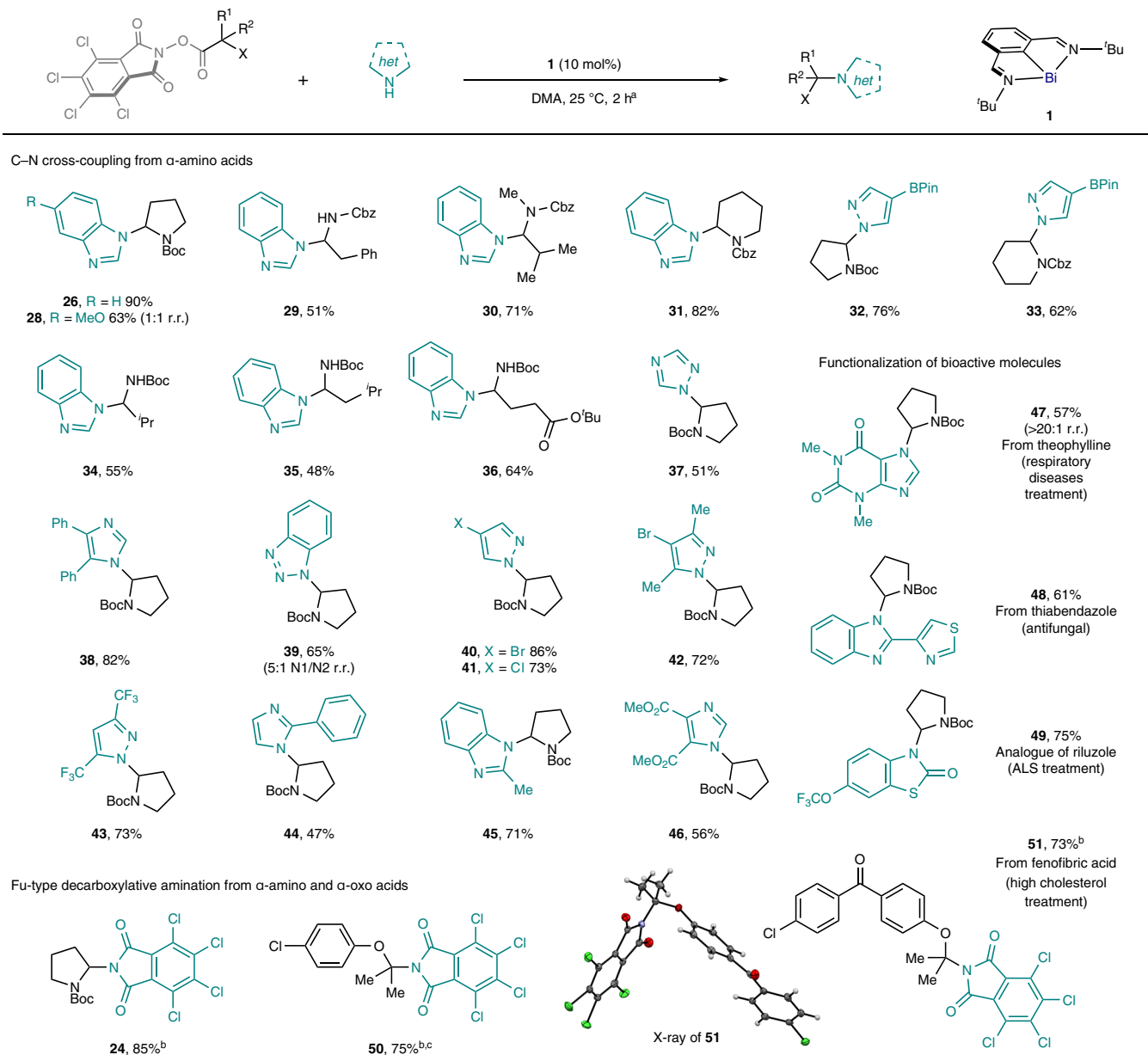
voltammometry recorded in  $MeCN$ , potential in V versus  $Fc^{0/+}$ . <sup>b</sup> Cyclic voltammometry recorded in  $MeCN$  (ref. 47); potential in V versus  $Fc^{0/+}$  converted from V versus saturated calomel electrode ( $-2.13$  V). <sup>c</sup> Yields and conversions determined by  $^1H$  NMR, unless noted otherwise. Ts, 4-toluenesulfonyl; MsO, mesylate.

where bismuth, besides emulating the redox behaviour of first-row transition metals during oxidative addition, allows the isolation and characterization of the corresponding alkyl–metal species resulting from radical recombination. We also found that, whereas classical  $S_N2$  reactivity is sensitive to steric effects (>24 h for **14**), single-electron oxidative addition of the corresponding RAE led to quantitative formation of complex **12** in <5 min. Furthermore, we found complexes **9**, **12** and **13** to be active by electron paramagnetic resonance (EPR) spectroscopy, especially upon light irradiation. Low-temperature EPR analysis of **12** suggests the formation of two radical species that decay

at different rates. This is consistent with the homolysis of the C–Bi bond (see Supplementary Information for details)<sup>41,42</sup>. To investigate this behaviour further, the reaction of bismuthinidene **1** with cyclopropylmethyl iodide was monitored by NMR at low temperature in the dark (Fig. 2c). Complete conversion into cyclopropylmethyl adduct **16** was observed within 1 h at  $-20$  °C. When the mixture was warmed to 50 °C, a slow but steady conversion to ring-opening compound **18** was observed (35% after 12 h).

This indicates that homolysis of the Bi–C bond in **16** takes place, leading to an in-cage radical pair (**int-1**). Furthermore, subjecting a

Table 1 | Scope of the C–N coupling reaction



<sup>a</sup>Reaction conditions: RAE (1 equiv., usually 0.2 mmol) and N-nucleophile (3 equiv.) in the presence of bismuthinidene **1** (10 mol%) in DMA (0.033 M) at 25 °C for 2 h. <sup>b</sup>In the absence of an external N-nucleophile. <sup>c</sup>DMA/MeCN 1:1 (0.05 M) as solvent. r.r., ratio of regioisomers. R<sup>1</sup> and R<sup>2</sup>, alkyl groups; X, N or O; Boc, *tert*-butoxycarbonyl; Cbz, benzyloxycarbonyl; BPin, pinacolboranyl; ALS, amyotrophic lateral sclerosis.

solution of **16** to blue light-emitting diode (LED) irradiation resulted in complete conversion into open product **18** within 5 min, showing that light can accelerate the radical ring-opening process<sup>25</sup>. Conversely, when cyclopropylmethyl RAE **17** was reacted with bismuthinidene **1**, a complex analogous to **16** was not observed; instead, radical ring-opening product **19** was immediately obtained, even in the dark. This is consistent with the two distinct mechanistic scenarios for the oxidative addition. On one hand, polar S<sub>N</sub>2-type reaction of cyclopropylmethyl iodide with **1** initially leads to **16**, which eventually ring-opens via alkyl-radical formation. On the other hand, SET and fragmentation of RAE **17** lead to an in-cage bismuth(II)/alkyl radical pair (**int-1**), for which cyclopropane ring-opening is faster than radical recombination, resulting in the formation of **19** (Fig. 2b). This alkyl radical-type reactivity is consistent with the behaviour displayed by these complexes: the secondary alkyl radical derived from **13** reacts with Michael

acceptors such as phenylvinylsulfone giving Giese addition product **21**, either in the dark (57%) or under blue-light irradiation (85%) (Fig. 3a, left). Additionally, the alkyl fragment of several complexes reacted with (2,2,6,6-tetramethylpiperidin-1-yl)oxyl radical (TEMPO) leading to C(sp<sup>3</sup>)-TEMPO adducts. Moreover, we observed that catalytic amounts of **1** can promote Giese-type reactions, among others, upon blue-light irradiation (Supplementary Information)<sup>43</sup>. When investigating the stability of the Bi(III)-alkyl compounds in solution, it was found that benzyl bismuth(III) complex **9** was especially sensitive to light irradiation, resulting in decomposition mainly to benzyl-benzyl dimers and unselective benzylation of the N,C,N ligand. On the other hand, complex **13** was stable in solution, even after 3 days at 60 °C (Fig. 2b)<sup>44</sup>. However, under blue-LED irradiation, **13** underwent slow but clean conversion into elimination product **15** and Bi(I), in a radical-type elimination reminiscent of that of alkylcobaloximes<sup>45</sup>. Furthermore,

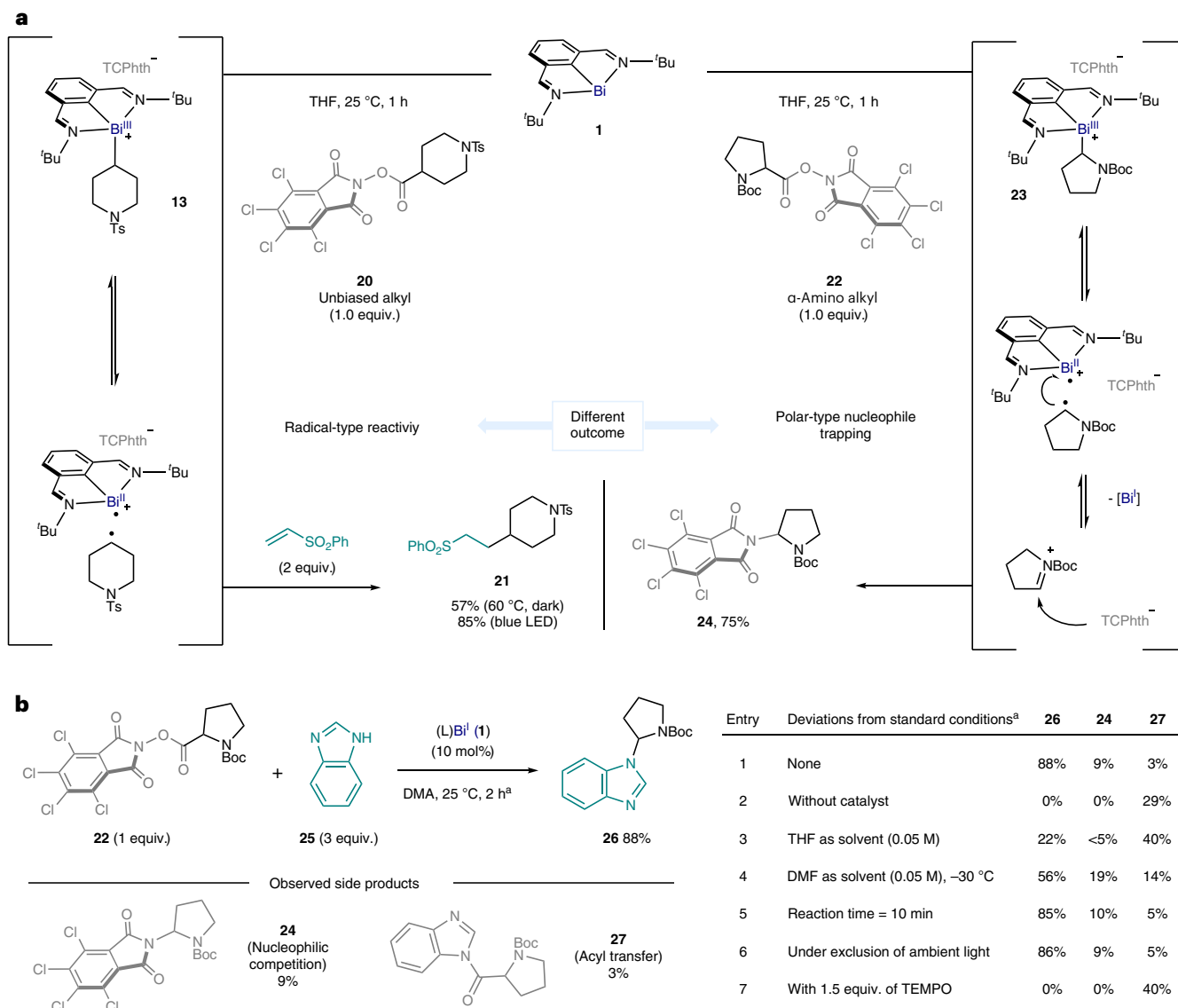


**Fig. 3 | Divergent reactivity of an unbiased alkyl-bismuth complex and an  $\alpha$ -amino alkyl-bismuth complex.** **a**, Stable unbiased alkyl-bismuth(III) intermediates displaying typical alkyl-radical reactivity (left) and unstable  $\alpha$ -amino alkyl-bismuth(III) complexes that evolve into iminium ion intermediates upon release of bismuth(I) (right). **b**, Development of a bismuth-catalysed

C–N cross-coupling reaction based on the oxidation of  $\alpha$ -amino alkyl radicals.

<sup>a</sup>Standard reaction conditions: **22** (1 equiv.) and **25** (3 equiv.) in the presence of bismuthinidene **1** (10 mol%) in DMA (0.033 M) at 25 °C for 2 h. Yields determined by <sup>1</sup>H NMR using diphenylmethane as internal standard. Ts, 4-toluenesulfonyl; Boc, *tert*-butoxycarbonyl.

scrambling experiments confirm that the exchange of alkyl fragments between two different Bi(III) adducts is also possible (Supplementary Information). Interestingly, when attempting the isolation of  $\alpha$ -amino alkyl-bismuth(III) adduct **23** derived from proline, we observed the exclusive formation of the product of decarboxylative amination **24**, with recovery of bismuthinidene **1** (Fig. 3a, right)<sup>30,33</sup>. It was speculated that product **24** would arise from the oxidation of the corresponding  $\alpha$ -amino alkyl radical by a highly reactive bismuth(II) species. This would lead to the formation of an electrophilic iminium ion<sup>28</sup>, which ultimately reacts with the TCPht anion to make the C–N bond (Fig. 4 and Supplementary Information).

At this point, it was envisaged that this reactivity could exploit the resulting iminium intermediates with external N-nucleophiles, leading to a formal C–N cross-coupling reaction. After optimization of the conditions, we found that the reaction of RAE **22** with 3 equiv. of benzimidazole (**25**) in the presence of 10 mol% of **1** in dimethylacetamide (DMA) at 25 °C afforded the product of C–N cross-coupling (**26**) in 88%

yield within 2 h (Fig. 3b). Under these conditions, the only observed side products were **24** (nucleophilic competition by TCPht) and the expected amide bond-formation product **27**, which could be minimized by controlling the stoichiometry and selecting the appropriate solvent (Fig. 3b, entry 1 versus entry 3) (see Supplementary Information for optimization details). Control experiments without the Bi catalyst led exclusively to the acyl-transfer product (Fig. 3b, entry 2). The high efficiency of the optimized reaction relies on the faster kinetics of the Bi-catalysed radical reaction compared to the background amide formation. For example, the reaction could be carried out at -30 °C in DMF (Fig. 3b, entry 4) or at room temperature in DMA in only 10 min (Fig. 3b, entry 5), giving the desired product in 56 and 85% yield, respectively. To exclude completely the requirement of photoexcitation for any of the steps of the transformation to proceed, the reaction was carried out under exclusion of ambient light, giving comparable results (Fig. 3b, entry 6). As expected, the addition of TEMPO completely inhibited the reaction (Fig. 3b, entry 7)<sup>41</sup>. Other bismuth(I) complexes



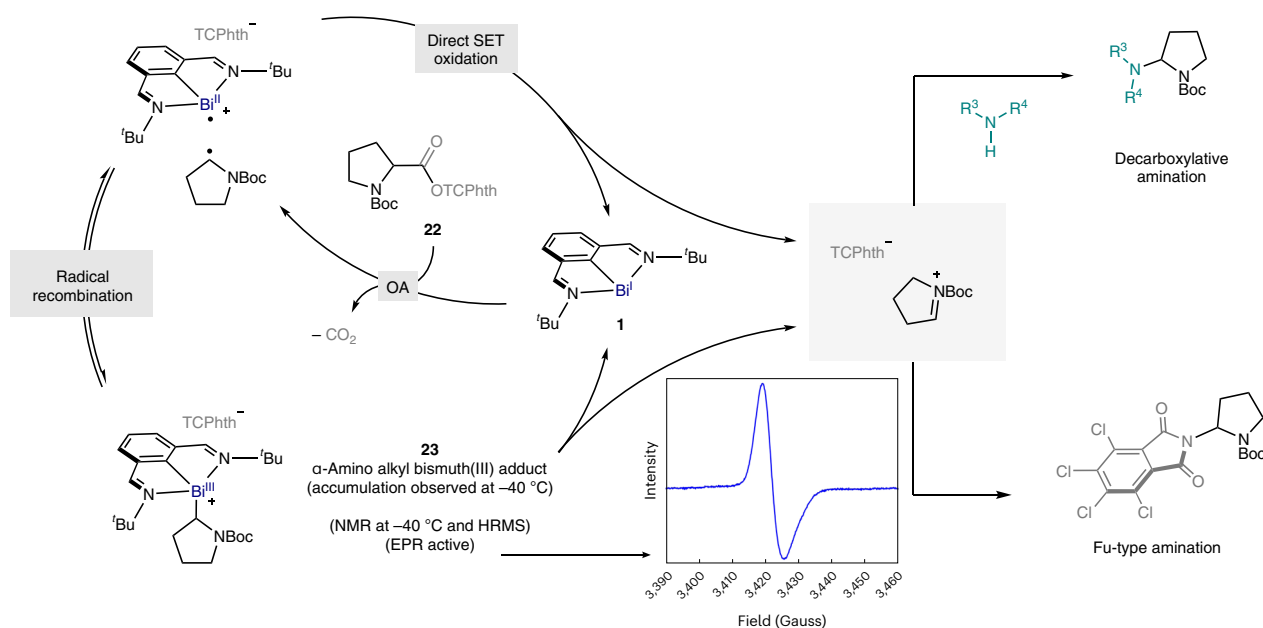


**Fig. 4 | Proposed mechanistic rationale.** The C–N cross-coupling reaction of  $\alpha$ -amino and  $\alpha$ -oxo acids via bismuth(I)-catalysed SET. The graph shows EPR analysis of **23**.  $\text{R}^3\text{R}^4\text{NH}$ , NH-heterocycle; OA, oxidative addition; Boc, *tert*-butoxycarbonyl.

and different redox couples tested led to decreased yields or inactivity, thus highlighting the importance of the finely tuned redox properties of **1** (Supplementary Information).

This methodology led us to the assembly of a wide variety of products containing an aminal- or a hemiaminal-ether structural motif, which would be challenging to construct from the parent halide (Table 1). RAEs of readily available natural and non-natural  $\alpha$ -amino acids were investigated (either fully protected or with free N–H bonds) as electrophilic partners. C–N coupling products derived from proline (**26**), phenylalanine (**29**), valine (**30** and **34**), leucine (**35**), glutamic acid (**36**) or pipercolic acid (**32** and **33**) were successfully obtained in good to excellent yields. Synthetically relevant N-heterocycles bearing free N–H bonds were evaluated. Using proline-derived RAE **22**, the corresponding C–N products of benzimidazoles (**26**, **28** and **45**), triazole (**37**), imidazoles (**38**, **44** and **46**) and pyrazoles (**32**, **33** and **40–43**) were obtained.

Non-symmetrical heterocycles such as benzotriazole (to give **39**) could also be accommodated, providing the product in a 5:1 N1/N2 ratio of regioisomers. A range of functional groups with different electronic properties were also tolerated (to give **43**, **46** and **50**). Since the radical process is orthogonal to classical transition-metal-catalysed cross-coupling reactions, different heteroaryl halides (to give **40–42**) and heteroaryl boronic esters (to give **32** and **33**) could be well tolerated. The strategy was successfully applied in the modification of bioactive molecules, such as theophylline (to give **47**, 57%, single regioisomer). The successful coupling using thiabendazole (to give **48**, 61%) provides another illustrative example of the orthogonal reactivity to transition metals, as the Lewis-basic sites on both starting material and product could inhibit catalysis by binding to a metal centre. Interestingly, carbamate-like N–H bonds could also be accommodated as demonstrated by the preparation of **49**, a hydroxylated analogue of riluzole. In the absence of external nucleophiles, the product of decarboxylative amination via formal  $\text{CO}_2$  extrusion was obtained. For this process, both  $\alpha$ -amino RAEs and  $\alpha$ -oxo RAEs reacted, giving hemiaminal-ether structures such as **50** and **51** in good yields. Overall, this strategy is complementary to the photochemical protocol reported by Fu and co-workers<sup>30</sup>, allowing the use of  $\alpha$ -heteroatom RAEs instead of unbiased alkyl substrates.

To shed light on the mechanism, we monitored the catalytic reaction of  $\alpha$ -amino RAE **22** by NMR with 10 mol% of **1** at  $-40^\circ\text{C}$ , using  $\text{DMF-d}_7$  as the solvent. In this scenario, the pair of rotamers of  $\alpha$ -amino alkyl-bismuth(III) intermediate **23** accumulated upon consumption of the RAE, coexisting with bismuthinidene **1**. It is important to mention that complex **23** was characterized by reaction of **1** with **22** in a separate stoichiometric experiment (see Supplementary Information for details). The accumulated **23** decays into **1** after 1 h at  $-20^\circ\text{C}$  (Fig. 4, bottom, Bi(I/II/III) pathway). However, we observed that the consumption of RAE **22** to give decarboxylative-amination product **24** occurs at a higher rate than that of the former process (see Supplementary Information for details of kinetic analysis). Thus, an alternative pathway should be considered in which the corresponding in-cage radical pair reacts directly through SET, leading to the iminium cation upon regeneration of Bi(I) (Fig. 4, bottom, Bi(I/II) pathway)<sup>46</sup>. Alternatively, radical recombination of the aforementioned radical pair leads to some accumulation of **23**, which eventually collapses into the reaction product (**24**) and **1**. Overall, the radical oxidative addition appears to be the rate-limiting step of the dominant pathway, as suggested by the continuous presence of **1** throughout the entire course of the reaction. Importantly, low-temperature EPR-spectroscopy analysis allowed us to detect an intense single-line signal, in agreement with the presence of the corresponding  $\alpha$ -amino alkyl-radical fragment. This strong EPR signal was observed even in the dark. This is consistent with the fact that the Bi(I/II) pair can promote this reactivity in the absence of external light irradiation.

## Conclusions

In summary, we have developed a radical oxidative addition of redox-active carbon electrophiles to low-valency bismuth, based on the SET from a well-defined Bi(I) complex to alkyl RAEs and Ks, allowing us to merge one- and two-electron reactivity in a single main-group element platform. This process led to a family of alkyl-bismuth(III) compounds, which were found to behave as equilibrium complexes with the corresponding in-cage radical pair formed by bismuth(II) and a free alkyl radical. Unbiased alkyl-bismuth(III) complexes are stable and can be characterized both in solution and in the solid state. On the other hand,  $\alpha$ -amino alkyl-bismuth(III) intermediates collapse

back into bismuth(I) upon releasing iminium cations, which can be trapped by external N-nucleophiles. This led to the development of a bismuth-catalysed C–N cross-coupling reaction, using complex N-heterocyclic compounds. This new type of radical catalysis is promoted by bismuth in an autonomous manner, through a radical Bi(I/II) or Bi(I/II/III) redox cycle, without the need for a photoredox system, a chemical oxidant, an external base or an electrochemical set-up. Overall, these findings open up a field of radical couplings by a main-group element and pave the way for the design of synthetically relevant transformations based on Bi radical catalysis.

## Online content

Any methods, additional references, Nature Portfolio reporting summaries, source data, extended data, supplementary information, acknowledgements, peer review information; details of author contributions and competing interests; and statements of data and code availability are available at <https://doi.org/10.1038/s41557-023-01229-7>.

## References

1. de Meijere, A. et al. (eds) *Metal-Catalyzed Cross-Coupling Reactions and More* (Wiley-VCH, 2013).
2. Smith, J. M., Harwood, S. J. & Baran, P. S. Radical retrosynthesis. *Acc. Chem. Res.* **51**, 1807–1817 (2018).
3. Yi, H. et al. Recent advances in radical C–H activation/radical cross-coupling. *Chem. Rev.* **117**, 9016–9085 (2017).
4. Yan, M., Lo, J. C., Edwards, J. T. & Baran, P. S. Radicals: reactive intermediates with translational potential. *J. Am. Chem. Soc.* **138**, 12692–12714 (2016).
5. Fawcett, A. et al. Photoinduced decarboxylative borylation of carboxylic acids. *Science* **357**, 283–286 (2017).
6. Fu, M.-C., Shang, R., Zhao, B., Wang, B. & Fu, Y. Photocatalytic decarboxylative alkylations mediated by triphenylphosphine and sodium iodide. *Science* **363**, 1429–1434 (2019).
7. Liu, W. et al. A biomimetic  $S_{\text{H}}2$  cross-coupling mechanism for quaternary  $sp^3$ -carbon formation. *Science* **374**, 1258–1263 (2021).
8. Zhang, B. et al. Ni-electrocatalytic  $C(sp^3)$ – $C(sp^3)$  doubly decarboxylative coupling. *Nature* **606**, 313–318 (2022).
9. Liu, Y. et al. Electrochemical C–N bond activation for deaminative reductive coupling of Katritzky salts. *Nat. Commun.* **12**, 6745 (2021).
10. Qin, T. et al. A general alkyl-alkyl cross-coupling enabled by redox-active esters and alkylzinc reagents. *Science* **352**, 801–805 (2016).
11. Murarka, S. *N*-(Acyloxy)phthalimides as redox-active esters in cross-coupling reactions. *Adv. Synth. Catal.* **360**, 1735–1753 (2018).
12. Weix, D. J. Methods and mechanisms for cross-electrophile coupling of  $Csp^2$  halides with alkyl electrophiles. *Acc. Chem. Res.* **48**, 1767–1775 (2015).
13. Choi, J. & Fu, G. C. Transition metal-catalyzed alkyl-alkyl bond formation: Another dimension in cross-coupling chemistry. *Science* **356**, eaaf7230 (2017).
14. Power, P. P. Main-group elements as transition metals. *Nature* **103**, 789–809 (2010).
15. Lipshultz, J. M., Li, G. & Radosevich, A. T. Main group redox catalysis of organopnictogens: vertical periodic trends and emerging opportunities in group 15. *J. Am. Chem. Soc.* **143**, 1699–1721 (2021).
16. Shibutani, S. et al. Organophotoredox-catalyzed decarboxylative  $C(sp^3)$ –O bond formation. *J. Am. Chem. Soc.* **142**, 1211–1216 (2020).
17. Moon, H. W. & Cornella, J. Bismuth redox catalysis: an emerging main-group platform for organic synthesis. *ACS Catal.* **12**, 1382–1393 (2022).
18. Planas, O., Wang, F., Leutzsch, M. & Cornella, J. Fluorination of arylboronic esters enabled by bismuth redox catalysis. *Science* **367**, 313–317 (2020).
19. Planas, O., Peciukenas, V. & Cornella, J. Bismuth-catalyzed oxidative coupling of arylboronic acids with triflate and nonaflate Salts. *J. Am. Chem. Soc.* **142**, 11382–11387 (2020).
20. Pang, Y. et al. Catalytic hydrodefluorination via oxidative addition, ligand metathesis, and reductive elimination at Bi(I)/Bi(III) centers. *J. Am. Chem. Soc.* **143**, 12487–12493 (2021).
21. Wang, F., Planas, O. & Cornella, J. Bi(I)-catalyzed transfer-hydrogenation with ammonia-borane. *J. Am. Chem. Soc.* **143**, 4235–4240 (2019).
22. Power, P. P. Persistent and stable radicals of the heavier main group elements and related species. *Chem. Rev.* **103**, 789–810 (2003).
23. Helling, C. & Schulz, S. Long-lived radicals of the heavier group 15 elements arsenic, antimony, and bismuth. *Eur. J. Inorg. Chem.* **2020**, 3209–3221 (2020).
24. Yamago, S. et al. Highly controlled living radical polymerization through dual activation of organobismuthines. *Angew. Chem. Int. Ed.* **46**, 1304–1306 (2007).
25. Ramler, J., Krummenacher, I. & Lichtenberg, C. Bismuth compounds in radical catalysis: transition metal bismuthanes facilitate thermally induced cycloisomerizations. *Angew. Chem. Int. Ed.* **58**, 12924–12929 (2019).
26. Schwamm, R. J. Isolation and characterization of a bismuth(II) radical. *Angew. Chem. Int. Ed.* **54**, 10630–10633 (2015).
27. Shono, T., Matsumura, Y. & Tsubata, K. Electroorganic chemistry. 46. A new carbon–carbon bond forming reaction at the  $\alpha$ -position of amines utilizing anodic oxidation as a key step. *J. Am. Chem. Soc.* **103**, 1172–1176 (1981).
28. Yamamoto, K., Kuriyama, M. & Onomura, O. Shono-type oxidation for functionalization of N-heterocycles. *Chem. Rec.* **21**, 2239–2253 (2021).
29. Ruiz-Castillo, P. & Buchwald, S. L. Applications of palladium-catalyzed C–N cross-coupling reactions. *Chem. Rev.* **116**, 12564–12649 (2016).
30. Zhao, W., Wurz, R. P., Peters, J. C. & Fu, G. C. Photoinduced, copper-catalyzed decarboxylative C–N coupling to generate protected amines: an alternative to the Curtius rearrangement. *J. Am. Chem. Soc.* **139**, 12153–12156 (2017).
31. Mao, R., Frey, A., Balon, J. & Hu, X. Decarboxylative  $C(sp^3)$ –N cross-coupling via synergetic photoredox and copper catalysis. *Nat. Catal.* **1**, 120–126 (2018).
32. Liang, Y., Zhang, X. & MacMillan, D. W. C. Decarboxylative  $sp^3$  C–N coupling via dual copper and photoredox catalysis. *Nature* **559**, 83–88 (2018).
33. Bosque, I. & Bach, T. 3-Acetoxyquinuclidine as catalyst in electron donor–acceptor complex-mediated reactions triggered by visible light. *ACS Catal.* **9**, 9103–9109 (2019).
34. Shao, X. et al. Decarboxylative  $C_{sp^3}$ –N bond formation by electrochemical oxidation of amino acids. *Org. Lett.* **21**, 9262–9267 (2019).
35. Sheng, T. et al. Electrochemical decarboxylative *N*-alkylation of heterocycles. *Org. Lett.* **22**, 7594–7598 (2020).
36. Kong, D., Moon, P. J., Bsharat, O. & Lundgren, R. J. Direct catalytic decarboxylative amination of aryl acetic acids. *Angew. Chem. Int. Ed.* **59**, 1313–1319 (2020).
37. Simon, P. et al. Monomeric organoantimony(I) and organobismuth(I) compounds stabilized by an NCN chelating ligand: syntheses and structures. *Angew. Chem. Int. Ed.* **49**, 5468–5471 (2010).
38. Lichtenberg, C. Well-defined, mononuclear Bi<sup>I</sup> and Bi<sup>II</sup> compounds: towards transition-metal-like behavior. *Angew. Chem. Int. Ed.* **55**, 484–486 (2016).
39. Hejda, M. et al. Probing the limits of oxidative addition of  $C(sp^3)$ –X bonds toward selected *N,C,N*-chelated bismuth(I) compounds. *Organometallics* **39**, 4320–4328 (2020).

40. Romero, N. A., Margrey, K. A., Tayand, N. E. & Nicewicz, D. A. Site-selective arene C–H amination via photoredox catalysis. *Science* **349**, 1326–1330 (2015).
41. Schwamm, R. J., Lein, M., Coles, M. P. & Fitchett, C. M. Catalytic oxidative coupling promoted by bismuth TEMPO<sub>2</sub> complexes. *Chem. Commun.* **54**, 916–919 (2018).
42. Yang, X. et al. Radical activation of N–H and O–H bonds at bismuth(II). *J. Am. Chem. Soc.* **144**, 16535–16544 (2022).
43. Qin, T. et al. Nickel-catalyzed Barton decarboxylation and Giese reactions: a practical take on classic transforms. *Angew. Chem. Int. Ed.* **56**, 260–265 (2017).
44. Cheng, W.-M., Shang, R. & Fu, Y. Irradiation-induced palladium-catalyzed decarboxylative desaturation enabled by a dual ligand system. *Nat. Commun.* **9**, 5215 (2018).
45. Sun, X., Chen, J. & Ritter, T. Catalytic dehydrogenative decarboxyolefination of carboxylic acids. *Nat. Chem.* **10**, 1229–1233 (2018).
46. Barry, J. T., Berg, D. J. & Tyler, D. R. Radical cage effects: comparison of solvent bulk viscosity and microviscosity in predicting the recombination efficiencies of radical cage pairs. *J. Am. Chem. Soc.* **138**, 9389–9392 (2016).
47. Isse, A. A. et al. Relevance of electron transfer mechanism in electrocatalysis: the reduction of organic halides at silver electrodes. *Chem. Commun.* 344–346 (2006).

**Publisher's note** Springer Nature remains neutral with regard to jurisdictional claims in published maps and institutional affiliations.

**Open Access** This article is licensed under a Creative Commons Attribution 4.0 International License, which permits use, sharing, adaptation, distribution and reproduction in any medium or format, as long as you give appropriate credit to the original author(s) and the source, provide a link to the Creative Commons license, and indicate if changes were made. The images or other third party material in this article are included in the article's Creative Commons license, unless indicated otherwise in a credit line to the material. If material is not included in the article's Creative Commons license and your intended use is not permitted by statutory regulation or exceeds the permitted use, you will need to obtain permission directly from the copyright holder. To view a copy of this license, visit <http://creativecommons.org/licenses/by/4.0/>.

© The Author(s) 2023



## Methods

### General procedure for the stoichiometric oxidative additions

Unless otherwise specified, a Schlenk flask with a magnetic stirring bar was charged, in an argon-filled glovebox, with bismuth complex **1** (1 equiv.) and the corresponding electrophile (1–2 equiv.). Both materials were dissolved in dry and degassed MeCN or THF (0.05 M) and the mixture was stirred until full discolouration of the characteristic dark green colour of bismuth complex **1** was observed, giving a homogeneous yellow/orange solution. After removal of the solvent in high vacuum, the corresponding oxidative-addition adduct was obtained as a pale yellow/orange air-sensitive solid. For characterization purposes, the same reactions can also be conducted directly in dry and degassed MeCN- $d_3$  or THF- $d_8$ .

### General procedure for the C–N coupling reaction

Unless otherwise specified, a 10 ml screw-cap vial with a magnetic stirring bar was charged with an RAE (1 equiv., usually 0.2 mmol) and the corresponding nucleophile (3 equiv.). The vial was placed in an argon-filled glovebox, where bismuth complex **1** (10 mol%) was added. Finally, everything was dissolved in anhydrous DMA (0.033 M). Then the vial was closed, taken outside the glovebox and stirred for 2 h at room temperature. After this time, the mixture was diluted in water and EtOAc. Then the organic fraction was washed twice with water and once with brine, dried over anhydrous  $\text{Na}_2\text{SO}_4$ , filtered and concentrated in vacuum. Finally, the product was purified using flash column chromatography or preparative thin-layer chromatography in silica gel.

### Data availability

The Supplementary Information contains all experimental procedures and analytical data ( $^1\text{H}$  NMR,  $^{19}\text{F}$  NMR,  $^{13}\text{C}$  NMR, HRMS and crystallographic data) for all new compounds. Electrochemical, EPR and kinetic data are also included, together with details of the optimization and mechanistic investigations. Crystallographic data for compounds **9** (CCDC 2178464), **11** (CCDC 2178465) and **51** (CCDC 2178503) can be downloaded free of charge from the Cambridge Crystallographic Data Centre [www.ccdc.cam.ac.uk](http://www.ccdc.cam.ac.uk).

### Acknowledgements

Financial support for this work was provided by the Max-Planck-Gesellschaft, the Max-Planck-Institut für Kohlenforschung, the Max-Planck-Institute for Chemical Energy Conversion

(EPR spectroscopy) and Fonds der Chemischen Industrie (FCI–VCI). We thank the European Research Council (ERC Starting Grant No. 850496) and the European Union's Horizon Europe research and innovation programme for a Marie Skłodowska-Curie postdoctoral fellowship to M.M. (MSCA-IF Grant No. 101062098). We thank the Institute of Chemical Research of Catalonia for an ICIQ-Severo Ochoa International Mobility grant to D.S. We thank the NMR, MS and X-ray departments of the Max-Planck-Institut für Kohlenforschung for analytical support. We thank N. Nöthling for X-ray crystallographic analysis. We especially thank A. Fürstner for insightful discussions and generous support.

### Author contributions

M.M. and D.S. developed the radical oxidative additions and studied the properties and reactivity of the resulting alkyl-bismuth adducts. M.M. developed the C–N cross-coupling reaction and prepared the Supplementary Information. M.L. conducted the kinetic studies and helped with the characterization of compounds using NMR spectroscopy. H.W.M. conducted electrochemical analysis. E.R. conducted EPR-spectroscopy analysis. J.C. and M.M. conceived the idea and prepared the manuscript. J.C. directed the project.

### Funding

Open access funding provided by Max Planck Society.

### Competing interests

The authors declare no competing interests.

### Additional information

**Supplementary information** The online version contains supplementary material available at <https://doi.org/10.1038/s41557-023-01229-7>.

**Correspondence and requests for materials** should be addressed to Josep Cornella.

**Peer review information** *Nature Chemistry* thanks Eun Jin Cho, Thierry Ollevier and the other, anonymous, reviewer(s) for their contribution to the peer review of this work.

**Reprints and permissions information** is available at [www.nature.com/reprints](http://www.nature.com/reprints).